BIOCHEMISTRY
including biophysical chemistry & molecular biology

Article

pubs.acs.org/biochemistry

Using Substrate Analogues To Probe the Kinetic Mechanism and Active Site of *Escherichia coli* MenD

Maohai Fang, Andrea Macova, Kimberly L. Hanson, Jillian Kos, and David R. J. Palmer*

Department of Chemistry, University of Saskatchewan, 110 Science Place, Saskatoon, SK S7N 5C9, Canada

ABSTRACT: MenD catalyzes the thiamin diphosphate-dependent decarboxylative carboligation of α-ketoglutarate and isochorismate. The enzyme is essential for menaquinone biosynthesis in many bacteria and has been proposed to be an antibiotic target. The kinetic mechanism of this enzyme has not previously been demonstrated because of the limitations of the UV-based kinetic assay. We have reported the synthesis of an isochorismate analogue that acts as a substrate for MenD. The apparent weaker binding of this analogue is advantageous in that it allows accurate kinetic experiments at substrate concentrations near K_m. Using this substrate in concert with the dead-end inhibitor methyl succinylphosphonate, an analogue of α-ketoglutarate, we show that MenD follows a ping-pong kinetic mechanism. Using both the natural and synthetic substrates, we have measured the effects of 12 mutations of residues at the active site. The results give experimental support to previous models and hypotheses and allow observations unavailable using only the natural substrate.

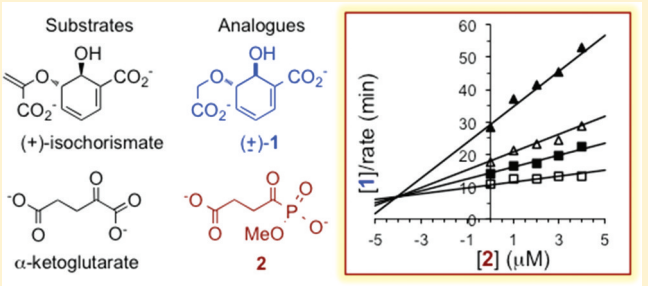

MenD is the designation for the enzyme 2-succinyl-5-enolpyruvyl-6-hydroxy-3-cyclohexene-1-carboxylate (SEPHCHC) synthase, which catalyzes the thiamin diphosphate (ThDP)- and Mg^{2+}-dependent reaction of isochorismate and α-ketoglutarate to form SEPHCHC and carbon dioxide.[1] The reaction is shown in Figure 1. This process is the first unique step in the biosynthetic pathway of menaquinone found in many bacteria.[2] Biosynthesis of menaquinone is essential for respiration in some bacterial pathogens such as *Mycobacterium tuberculosis*, particularly under low-oxygen conditions, and depletion of the menaquinone pool has been demonstrated as a means of deterring *M. tuberculosis* growth.[3−5] Enzymes from the menaquinone pathway have therefore been proposed as targets for drug development.[6−9]

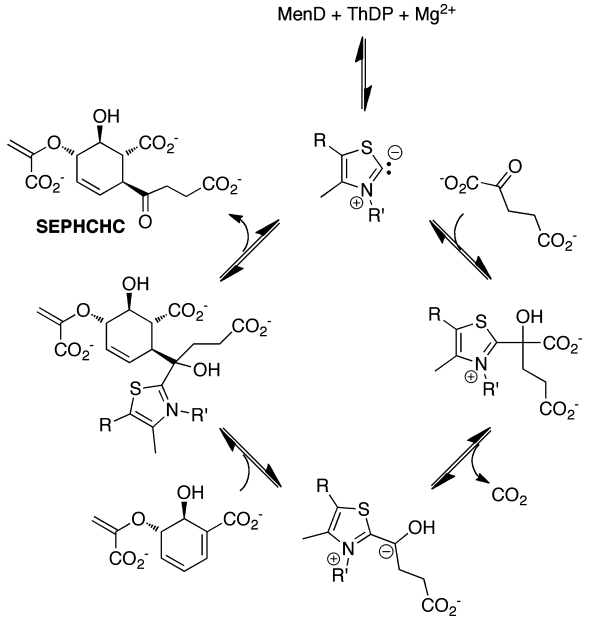

Figure 1. Proposed kinetic mechanism of the MenD-catalyzed reaction.

The MenD-catalyzed reaction has been studied for many years, mainly using the enzyme from *Escherichia coli*, although there has been considerable confusion regarding the nature of the reaction itself. MenD was for many years known as 2-succinyl-6-hydroxy-2,4-cyclohexadiene-1-carboxylate (SHCHC) synthase, because of the relatively facile elimination of pyruvate from SEPHCHC under basic conditions.[10−12] However, careful work in the laboratory of Z. Guo demonstrated that SEPHCHC is the product of the MenD-catalyzed reaction,[1,13,14] and the elimination of pyruvate is subsequently catalyzed by another enzyme, MenH. MenD belongs to a family of homologous ThDP-dependent enzymes that contain many conserved structural features, particularly in their binding of the coenzyme.[15,16] As illustrated in Figure 2, there are many examples of enzymes that catalyze a similar ThDP-dependent decarboxylation of a 2-oxo acid, but the resulting intermediate may be used in a variety of reactions.

MenD has been assumed to follow a classical, one-site ping-pong bi-bi kinetic mechanism, also termed a substituted-enzyme mechanism or double-displacement mechanism. Specifically, the enzyme-bound ThDP is deprotonated at C-2 of its thiazolium ring, which is used as a nucleophilic catalyst for

Received: August 2, 2011
Revised: September 2, 2011
Published: September 19, 2011

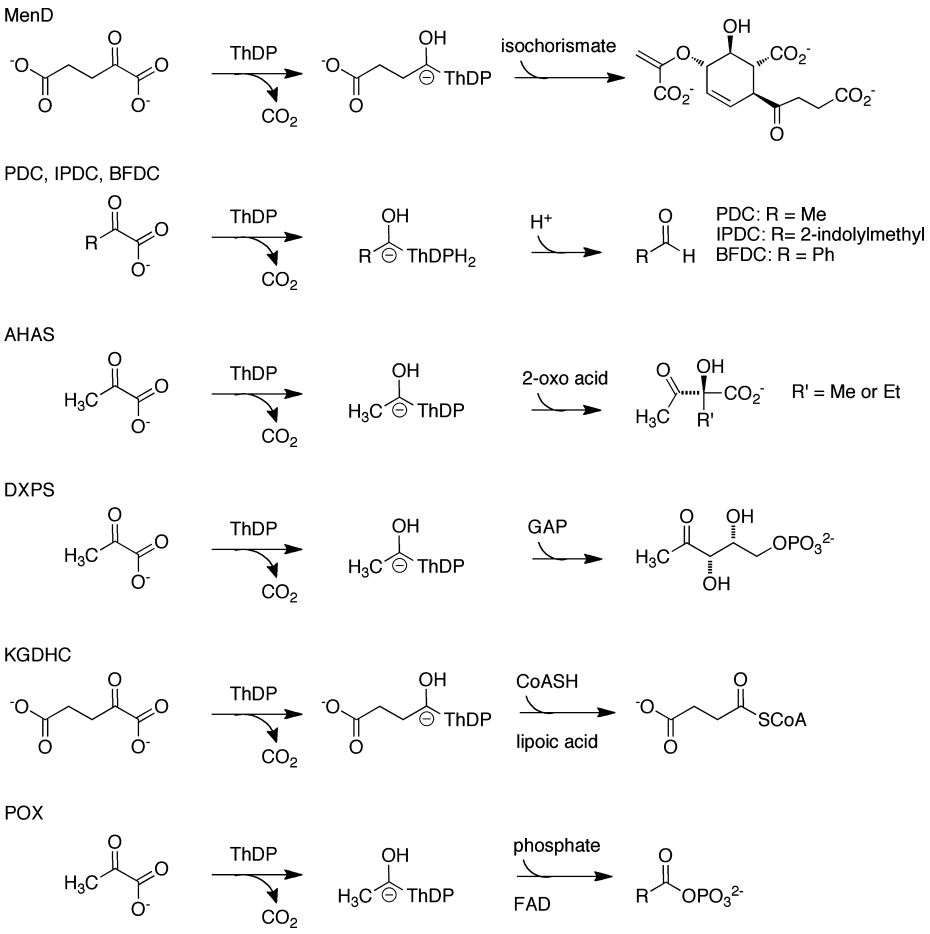

Figure 2. Reactions of several homologous ThDP-dependent decarboxylating enzymes. Note that for DXPS, the reaction is believed to follow a random sequential mechanism (see the text).

a canonical 2-oxo acid decarboxylation reaction of α-ketoglutarate. Isochorismate binds to the enzyme subsequent to this reaction, and a carboligation (comparable to a Stetter reaction) occurs between the β-carbon of isochorismate and the succinyl-ThDP, the product of which breaks down to generate SEPHCHC and regenerate the ThDP anion. This mechanism, shown in Figure 1, has never been demonstrated in experiments.

While most ThDP-dependent enzymes are considered to share a common kinetic mechanism,[17] this is not always the case. 1-Deoxy-D-xylulose 5-phosphate synthase (DXPS), for example, also catalyzes the ThDP-dependent decarboxylation of a 2-oxo acid, pyruvate. The resulting carbanion/enamine is then added to the carbonyl carbon of a second substrate, D-glyceraldehyde 3-phosphate (GAP). Eubanks and Poulter[18] showed that for the DXPS from *Rhodobacter capsulatus*, both substrates bound to the enzyme during catalysis. Subsequent work by Sisquella et al. with *E. coli* DXPS using single-molecule force spectroscopy also supported an ordered mechanism in which pyruvate binds tightly, and GAP binds before the reaction occurs.[19] This precedent within the enzyme family demonstrates that experimental evidence is required to establish the kinetic mechanism of MenD.

The proposed ping-pong mechanism can be supported by two well-established methods. First, double-reciprocal plots of one substrate at a series of concentrations of the other will result in a diagnostic pattern for this mechanism: a series of parallel lines. (Intersecting lines would be indicative of a sequential mechanism.) This set of experiments can be conducted properly only at concentrations around the K_m of each substrate. A second approach to establishing the kinetic mechanism is the use of a dead-end inhibitor. For example, a competitive analogue with respect to the first substrate would be uncompetitive with respect to the second in a ping-pong mechanism, but noncompetitive for ordered or random sequential mechanisms.[20] Dixon and Cornish–Bowden plots can be used together to diagnose these modes of inhibition, again using substrate concentrations above and below the K_m value.[21]

MenD is assayed by observation of the consumption of isochorismate, which can be monitored at 278 nm. The product of the reaction, SEPHCHC, has essentially no UV absorbance. The apparent K_m of isochorismate, as measured by our group and by others, is quite low (<1 μM[1,9]), and the extinction coefficient of isochorismate (8300 M^{-1} cm^{-1}[22]) is not sufficient to allow assay of the enzyme at concentrations near the K_m. This rules out both of the methods listed above for demonstrating the ping-pong mechanism.

Our lab recently reported the synthesis of an analogue of isochorismate that differs from the naturally occurring compound only in the enolpyruvyl substituent, which is replaced with a carboxymethyl group.[23] The resulting analogue, (±)-**1**, shown in Figure 3, is more stable than isochorismate. Only the (+)-isomer acts as a substrate for *E. coli* MenD, with an apparent K_m value (at a saturating concentration of α-ketoglutarate) of 12 μM. This substrate therefore provides an

dx.doi.org/10.1021/bi201202n | *Biochemistry* 2011, 50, 8712–8721

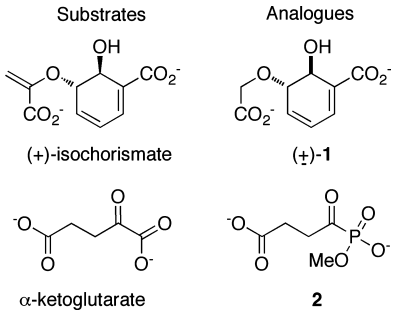

Figure 3. Substrates of MenD and the corresponding synthetic analogues. (±)-**1** is a racemic mixture of the *trans* isomer.

opportunity to support or disprove the proposed ping-pong mechanism.

We have also described a series of succinyl phosphonate esters that act as reversible, competitive inhibitors of MenD with respect to α-ketoglutarate by mimicking the substrate.[9] These compounds are proposed to bind to the active site and react with ThDP but not proceed forward to products by cleavage of the C−P bond. The closest of these analogues, and the best inhibitor of MenD, is the monomethyl succinylphosphonate ester, **2**, shown in Figure 3. The measured K_i value of **2** with respect to α-ketoglutarate is 700 nM. With this competitive inhibitor, we can use inhibition patterns with respect to **1** to evaluate the kinetic mechanism of MenD.

We anticipate that **1** will, despite the higher K_m value, behave in all other respects like isochorismate. Any differences in its interactions with the active site of the enzyme would be exhibited by comparing the behavior of the natural and synthetic substrates in the presence of active-site mutants. On the basis of sequence alignment comparisons with other ThDP-dependent enzymes, and the reported crystal structures of MenD, we constructed a series of MenD mutants. After these mutants were constructed, the catalytic activity of an overlapping set of mutants was reported for the MenD from *Bacillus subtilis*.[24] We have observed the effects of the mutations on the kinetic constants with respect to the natural substrates and cofactors, as well as the artificial substrate **1**, and used these results to enhance our understanding of the roles of these active-site residues and to compare the behavior of the enzymes from *B. subtilis* and *E. coli*.

MATERIALS AND METHODS

Syntheses of (±)-5-(carboxylatomethoxy)-6-hydroxycyclohexa-1,3-diene carboxylate (**1**) and sodium 4-(sodium, methylphosphono)-4-oxobutanoate (**2**) have been described previously.[9,23] Chemical reagents, including buffers, salts, and fine chemicals, were obtained from Sigma-Aldrich Canada, Ltd. (Oakville, ON) or VWR CanLab (Mississaugua, ON) and were categorized as molecular biology grade or were the highest grade available.

MenD and its mutants were produced and purified by the previously described procedures.[9] A different 1 mL Ni^{2+} affinity column was used for the purification of each mutant. All mutants were expressed like the wild-type enzyme.

Enzymatic assays were conducted as described previously, following the disappearance of either isochorismate or **1** at 278 nm.[9,23] The reaction rate was determined with 30 nM MenD, 100 mM Tris (pH 7.4), 5 mM $MgCl_2$, and 50 μM ThDP by varying the concentrations of α-ketoglutarate (4, 8, 16, 32, and 64 μM) with a constant concentration of **1** at 5, 10, 20, or 50 μM. Kinetic constants were determined using Leonora[25] by nonlinear least-squares fitting of data to eq 1, which describes the initial rate in the absence of products for a ping-pong bi-bi enzymatic reaction:

$$v = \frac{V_{max}[A][B]}{K_m^B[A] + K_m^A[B] + [A][B]} \quad (1)$$

where [A] is the concentration of the substrate (α-ketoglutarate) that first binds to MenD, [B] is the concentration of the second substrate (isochorismate or **1**), K_m^A and K_m^B are the Michaelis constants for substrates A and B, respectively, and V_{max} is the maximal velocity when both substrates are at saturating concentrations.

The apparent rate constants for each of the MenD variants with respect to each substrate or cofactor were determined at saturating concentrations of the other substrate(s) and cofactor(s), where possible. Saturating conditions were determined independently for each mutant. Kinetic constants were determined using Leonora[25] by nonlinear least-squares fitting of the data to the Michaelis−Menten equation (eq 2)

$$v = V_{max}[S]/(K_m + [S]) \quad (2)$$

where v is the measured rate, V_{max} is the apparent maximal rate, K_m is the apparent Michaelis constant, and [S] is the concentration of the varied substrate. The apparent turnover number, k_{cat}, is calculated from V_{max} by dividing by the enzyme concentration.

In cases where the apparent K_m of isochorismate was so high that experiments at substrate concentrations above K_m could not be performed because of absorbance values beyond the limits of the spectrophotometer, kinetic constants were estimated with a Hanes−Woolf plot ([S]/v vs [S]).

The dead-end competitive inhibition by **2** with respect to **1** was observed with α-ketoglutarate at a fixed nonsaturating concentration (~K_m). The inhibition of **2** with respect to **1** was similarly determined by a Dixon plot (1/v vs [**2**]) and a Cornish−Bowden plot ([**1**]/v vs [**2**]). The reaction rate was determined with 60 nM MenD, 100 mM Tris (pH 7.4), 5 mM $MgCl_2$, and 50 μM ThDP. The concentration of α-ketoglutarate was fixed at 6 μM, and concentrations of **1** were 3, 6, 9, and 18 μM. The concentrations of **2** used were 10, 20, 30, and 40 μM. The uncertainties reported for all rate constants are based on the error of the nonlinear fit.

Site-directed mutants were generated using the QuikChange mutagenesis kit (Strategene, La Jolla, CA) as described previously.[9] All mutants were confirmed by sequencing at the National Research Council Plant Biotechnology Institute DNA Technologies Unit (Saskatoon, SK).

RESULTS AND DISCUSSION

Determination of the Kinetic Mechanism Using 1. The proposed ping-pong bi-bi mechanism of the MenD-catalyzed reaction in Figure 1 shows α-ketoglutarate binding first to the enzyme, followed by ThDP-dependent decarboxylation. Only after carbon dioxide is released does productive binding of isochorismate occur. The double-reciprocal plot for such a mechanism is a set of parallel lines; that is, the apparent K_m/V_{max} would not change, because the reaction of isochorismate with the enzyme-bound succinyl-ThDP anion would affect the second-order rate constant of the decarboxylation reaction. Because the K_m of isochorismate is too low for that substrate to be used effectively in this experiment, the

approximately 10-fold higher apparent K_m of (+)-**1** was exploited to demonstrate the kinetic mechanism of MenD.

The results of the variation of the rate of the MenD-catalyzed reaction of α-ketoglutarate and (+)-**1** are shown in Figure 4.

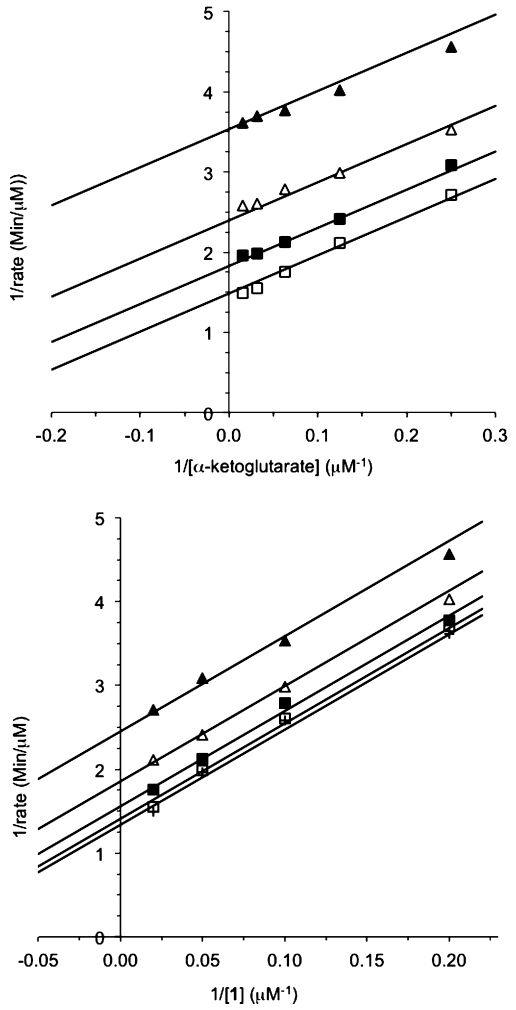

Figure 4. Lineweaver–Burk plots of the dependence of rate on varying substrate concentrations at pH 7.4 in the presence of 100 mM Tris, 5 mM $MgCl_2$, 50 μM ThDP, and 30 nM MenD: (top) variation with respect to the concentration of α-ketoglutarate with 4, 8, 16, 32, and 64 μM **1** and (bottom) variation with respect to the concentration of **1** with 5, 10, 20, and 50 μM α-ketoglutarate.

The parallel lines are consistent with the predicted ping-pong mechanism and represent the first such experimental evidence for MenD. Furthermore, these results give the "true" values for k_{cat} and K_m, to the extent that the concentrations of ThDP and Mg^{2+} can be considered saturating. The k_{cat} value (27 ± 2 min^{-1}) is just slightly higher than our previously reported apparent value using **1** as a substrate.[23] The K_m values for α-ketoglutarate and (+)-**1** are 3.8 ± 0.2 and 9.1 ± 0.4 μM, respectively, resulting in second-order rate constants of 1.2 × 10^5 and 5.0 × 10^4 M^{-1} s^{-1}, respectively, for these substrates. As previously noted, the turnover number for (+)-**1** is somewhat higher than the apparent k_{cat} observed for the isochorismate reaction. However, the apparent second-order rate constant with respect to isochorismate[9] is more than 3 times higher than that for the synthetic substrate analogue.

Inhibition of the MenD-Catalyzed Reaction of 1 by 2.

The α-ketoglutarate analogue **2** is a competitive inhibitor of the MenD reaction and very likely functions by binding to the active site and reacting with ThDP. The resulting adduct cannot decarboxylate, because the carboxyl moiety has been replaced with a methyl phosphonyl moiety (Figure 3). This behavior has been observed for phosphonate analogues with related ThDP-dependent enzymes.[26−29]

The mode of inhibition by **2** with respect to α-ketoglutarate in the reaction with **1** was not expected to change. Dixon and Cornish–Bowden plots, shown in Figure 5, were used to

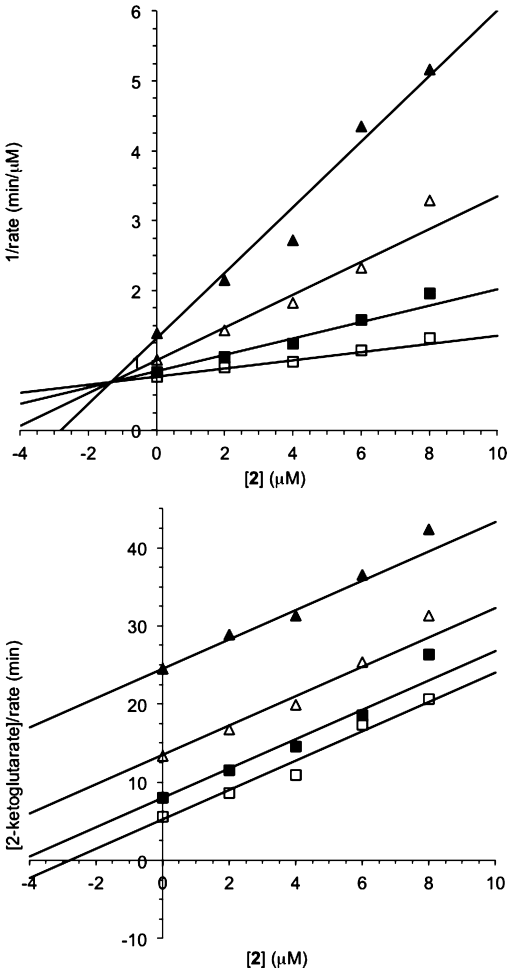

Figure 5. Variation of rate with inhibitor concentration of the MenD-catalyzed reaction of α-ketoglutarate and **1** in the presence of 100 mM Tris, 5 mM $MgCl_2$, 50 μM ThDP, 60 nM MenD, 100 μM **2**, and 4, 8, 16, or 32 mM α-ketoglutarate: (top) Dixon plot and (bottom) Cornish–Bowden plot. Patterns are consistent with competitive inhibition by **2** with respect to α-ketoglutarate.

evaluate the inhibition and determine the inhibition constant. As expected, the intersecting pattern of lines in the Dixon plot and parallel lines of the Cornish–Bowden plot unambiguously diagnose the inhibition as competitive. The K_i value was determined to be 1.3 ± 0.2 μM, comparable to the previously determined value for the reaction using isochorismate as the substrate.[9]

The mode of inhibition with respect to **1** was determined in the same manner, and the Dixon and Cornish–Bowden plots are shown in Figure 6. The parallel lines of the Dixon plot, coupled with the intersecting pattern of lines of the Cornish–Bowden plot, diagnose the mode of inhibition as uncompetitive

dx.doi.org/10.1021/bi201202n | Biochemistry 2011, 50, 8712–8721

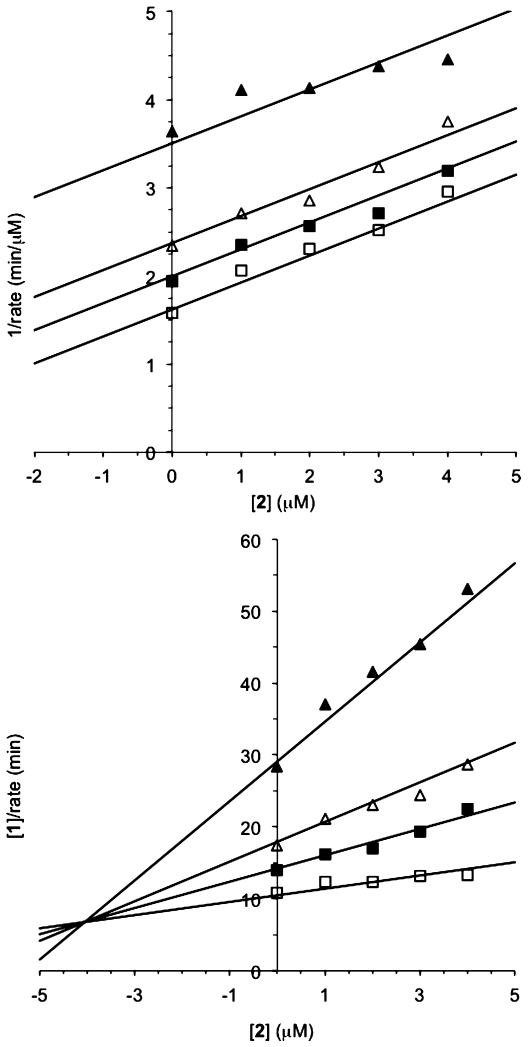

Figure 6. Variation of rate with inhibitor concentration of the MenD-catalyzed reaction of α-ketoglutarate and **1** in the presence of 100 mM Tris, 5 mM $MgCl_2$, 50 μM ThDP, 60 nM MenD, 6 μM α-ketoglutarate, and 3, 6, 9, and 18 mM **1**: (top) Dixon plot and (bottom) Cornish–Bowden plot. Patterns are consistent with uncompetitive inhibition by **2** with respect to **1**.

with respect to **1**. (Noncompetitive, or mixed, inhibition would give rise to an intersecting pattern of lines in both plots.[21]) The inhibition constant for **2** with respect to **1** was determined to be 4.1 ± 0.3 μM. The mode of inhibition fully supports the mechanism of Figure 1.

Site-Directed Mutagenesis. Sequence alignments of MenD sequences from a wide variety of bacteria, and alignments with sequences of structurally characterized ThDP-dependent 2-oxo acid decarboxylase enzymes, allowed the identification of conserved residues proposed to be important for catalysis.[12] The subsequent report of medium-resolution structures of MenD from *E. coli*[30] and *B. subtilis*[24] confirmed the sequence-based predictions, showing residues directly involved in the binding of ThDP and divalent metal ion. To date, there has been no structure with substrates bound in a meaningful way. MenD has been crystallized bound to α-ketoglutarate, but in the absence of ThDP, the resulting structure shows the substrate bound in the cofactor-binding site such that no reaction could occur.[31] Modeling of an isochorismate–succinyl-ThDP adduct in the active site[24,30] did suggest several residues that could be directly involved in substrate binding and/or catalysis. We chose a series of residues that are predicted to interact with the substrates and/or cofactors as targets for site-directed mutagenesis.

The effects of site-directed mutagenesis on each substrate and cofactor can be observed by determining the apparent kinetic constants with respect to each ligand at saturating concentrations of the others. In the case of MenD, we can see how changing a particular residue affects the binding and/or activation of ThDP, Mg^{2+}, α-ketoglutarate, and isochorismate. With this and the crystallographic information already available, the roles of active-site residues can be understood.

The Michaelis constant of isochorismate is a confounding factor, as described above. Because the K_m value is too low to be measured accurately using the spectrophotometric assay, only large increases in this value can be assessed accurately. The higher Michaelis constant of (+)-**1** addresses this problem satisfactorily, giving a better opportunity to observe effects on the Michaelis constant for the second substrate. Of course, a very large Michaelis constant also curtails available information. Because the rates are measured by observing the disappearance of the absorbance due to the second substrate, high concentrations result in absorbance values beyond the range of the spectrophotometer. While a high K_m value can be estimated satisfactorily by a Hanes–Woolf plot, the kinetic constants with respect to the other ligands cannot be measured in such a circumstance, because one cannot work at saturating concentrations of isochorismate (or **1**). In this respect, experiments with isochorismate and with **1** can provide complementary information. We also hoped to identify specific interactions that lead to the discrimination between the natural and the synthetic substrate.

Active-Site Arginine and Lysine Residues Arg33, Arg107, Lys292, Arg293, Arg395, and Arg413. The crystal structure of *E. coli* MenD[30] shows a pair of active sites at the interface of two monomers of the active dimeric protein. Each active site contains a collection of positively charged or basic residues surrounding an apparent substrate-binding pocket next to the bound cofactors, as shown in Figure 7. Given that the two substrates contain four carboxylate groups,

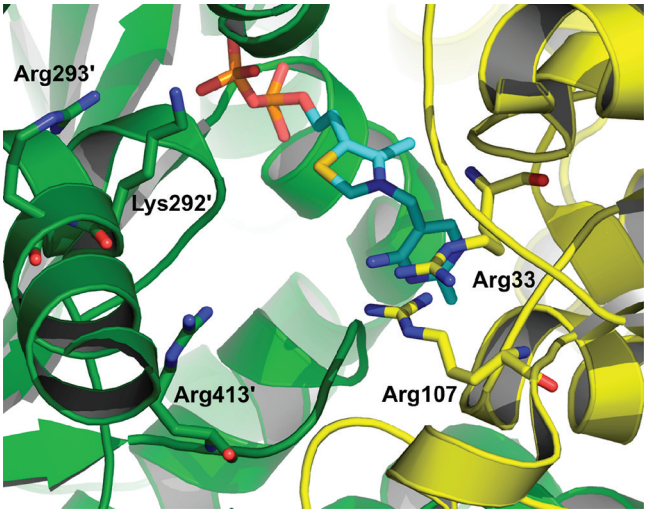

Figure 7. View of the active site of MenD. Monomers are shown with ribbon diagrams with carbon atoms colored yellow or green; ThDP is shown with carbon atoms colored cyan. The basic/positively charged residues studied by mutagenesis are shown. Structure coordinates were from Protein Data Bank entry 2JLC. This figure was generated with MacPyMOL (Shrödinger LLC).

an array of positive charges to bind and activate the reactants is not surprising. The subsequently determined structure of *B. subtilis* MenD[24] showed that residues Arg32, Arg106, Lys299, Arg409, and Arg428 of that enzyme correspond to Arg33, Arg107, Lys292, Arg395, and Arg413 of the *E. coli* enzyme, respectively, but Arg293, present at the active site of *E. coli* MenD, is not conserved in the *B. subtilis* enzyme. The same article reporting this structure also reports the results of mutating each of the five conserved residues to alanine. Briefly, these nonconservative mutations demonstrated that truncating the side chains of Arg32 and Arg106 had a significant impact on the binding and/or activation of isochorismate, altering Arg428 had a major impact on the interaction of α-ketoglutarate with the protein, while mutation of Arg409 affected both substrates. The K299A mutation had a relatively small effect, given the large change to the residue.

Our approach used more conservative substitutions in most cases, intended to allow subtle effects to be observed, but overall our results support the conclusions of Dawson et al.[24] The results are listed in Tables 1−4.

Table 1. Effects of Mutagenesis on Rate Constants with Respect to ThDP

	K_m (μM)	k_{cat} (min^{-1})	k_{cat}/K_m (min^{-1} μM^{-1})
WT	8 ± 1	17 ± 2	2.1 ± 0.1
S32A	4.3 ± 0.3	14 ± 1	3.2 ± 0.2
E55D	24 ± 4	13 ± 1	0.53 ± 0.06
R107K	4.8 ± 0.7	10 ± 1	2.2 ± 0.2
K292Q	2.0 ± 0.2	12 ± 1	6.0 ± 0.4
R293K	4.7 ± 0.3	18 ± 2	3.8 ± 0.1
S391A	17 ± 1	18 ± 1	1.0 ± 0.1
R395K	2.2 ± 0.2	7.9 ± 0.3	3.6 ± 0.2
R413K	5.0 ± 0.9	6.1 ± 0.3	1.2 ± 0.2

Table 2. Effects of Mutagenesis on Apparent Rate Constants with Respect to Mg^{2+}

	K_m (μM)	k_{cat} (min^{-1})	k_{cat}/K_m (min^{-1} μM^{-1})
WT	44 ± 1	17 ± 2	0.38 ± 0.04
S32A	80 ± 10	14 ± 1	0.17 ± 0.02
E55D	8 ± 2	13 ± 1	1.6 ± 0.3
R107K	49 ± 8	10 ± 1	0.21 ± 0.03
K292Q	2.6 ± 0.7	12 ± 1	5 ± 1
R293K	200 ± 100	18 ± 2	0.09 ± 0.04
S391A	13 ± 2	18 ± 1	1.4 ± 0.2
R395K	<2	7.9 ± 0.3	>4
R413K	10 ± 2	6.1 ± 0.3	0.61 ± 0.09
I418L	400 ± 80	13 ± 1	0.031 ± 0.005

Arg33 was mutated to glutamine and to lysine to differentiate the effects of maintaining hydrogen bonding (R33Q) and maintaining the possibility of a positive charge (R33K). Both mutations have a large and unfavorable impact on the Michaelis constant for isochorismate (Table 4), and the R33K mutation essentially kills activity in the presence of **1**. Interestingly, the R33Q mutant is a significantly better catalyst than the R33K mutant, suggesting that the residue may act through hydrogen bond donation more so than ionic interaction.

The mutation of Arg107 resulting in the R107K mutant also had a significant effect on the Michaelis constant of isochorismate, although to a lesser extent than R33K. The

Table 3. Effects of Mutagenesis on Apparent Rate Constants with Respect to α-Ketoglutarate

	K_m (μM)	k_{cat} (min^{-1})	k_{cat}/K_m (min^{-1} μM^{-1})
WT	9.9 ± 0.6	17 ± 2	1.7 ± 0.1
S32A	9.9 ± 0.2	14 ± 1	1.4 ± 0.2
E55D	12 ± 2	13 ± 1	1.1 ± 0.1
R107K	5.3 ± 0.9	10 ± 1	1.9 ± 0.5
K292Q	2.6 ± 0.3	12 ± 1	4.6 ± 0.4
R293K	9.1 ± 0.8	18 ± 2	2.0 ± 0.1
S391A	13 ± 1	18 ± 1	1.4 ± 0.1
R395K	45 ± 3	7.9 ± 0.3	0.18 ± 0.2
R413K	220 ± 40	6.1 ± 0.3	0.028 ± 0.004
I418L	200 ± 30	13 ± 1	0.063 ± 0.006

Table 4. Effects of Mutagenesis on Apparent Rate Constants with Respect to Isochorismate and (+)-1

	substrate	K_m (μM)	k_{cat} (min^{-1})	k_{cat}/K_m (min^{-1} μM^{-1})
WT	isochorismate	nd[a]	17 ± 2	~10
	(+)-**1**	12 ± 1	24 ± 2	2.0 ± 0.1
S32A	isochorismate	nd[a]	14 ± 1	−
	(+)-**1**	42 ± 2	15 ± 1	0.35 ± 0.01
S32D	isochorismate[b]	260	2.5	0.0095
	(+)-**1**		trace activity	
R33Q	isochorismate[b]	54	7.3	0.14
	(+)-**1**[b]	430	2.4	0.0056
R33K	isochorismate[b]	140	6.3	0.047
	(+)-**1**		trace activity	
R107K	isochorismate	7.5 ± 0.5	10 ± 1	1.3 ± 0.1
	(+)-**1**[b]	91	7.1	0.078
K292Q	isochorismate	nd[a]	12 ± 1	−
	(+)-**1**	50 ± 1	17 ± 1	0.34 ± 0.01
R293K	isochorismate	nd[a]	18 ± 1	−
	(+)-**1**	4.2 ± 0.7	24 ± 1	5.7 ± 0.7
S391A	isochorismate	nd[a]	18 ± 1	−
	(+)-**1**	36 ± 3	13 ± 1	0.36 ± 0.06
R395A	isochorismate[b]	36	2.6	0.07
	(+)-**1**[b]	390	2.4	0.0061
R395K	isochorismate	5.3 ± 0.9	7.9 ± 0.3	1.5 ± 0.2
	(+)-**1**[b]	109	11	0.10
R413K	isochorismate	nd[a]	13 ± 1	−
	(+)-**1**	10 ± 1	10 ± 1	1.0 ± 0.2
I418L	isochorismate	nd[a]	13 ± 1	−
	(+)-**1**	27 ± 3	23 ± 1	0.85 ± 0.06

[a]nd = not determined. As discussed in the text, the Michaelis constant for isochorismate is too low to be determined accurately, but has been estimated to be about 1 μM. [b]Value estimated by a Hanes−Woolf plot. Concentrations above K_m result in absorbance values beyond the range of the spectophotometer.

kinetic constants with respect to α-ketoglutarate and the two cofactors (Tables 1−3) are virtually unchanged for this mutant. The effect of this mutation on the K_m of (+)-**1** is essentially identical (Table 4), although it is of interest that this is one of the few mutations for which the turnover number is smaller for the artificial substrate, as also observed for R33Q. This corresponds with the in silico model of an isochorismate−succinyl-ThDP adduct in the active site, as constructed by Dawson and co-workers,[24] which shows the residues analogous to Arg33 and Arg107 interacting with the enolpyruvate moiety of isochorismate. It is this moiety that has been altered in the artificial substrate **1**, and thus, the effects of these mutations are

dx.doi.org/10.1021/bi201202n | *Biochemistry* 2011, 50, 8712−8721

different for the different substrates. The use of **1** has therefore provided the best support for the proposed mode of binding.

We have previously discussed the effects of mutating R395;[9] R395K shows an ~4-fold increase in its Michaelis constants for both α-ketoglutarate (Table 3) and the ThDP (Table 1), and a significant increase in the K_m of isochorismate to a measurable value (Table 4). Using the substrate **1**, we can quantitate the effects of this mutation effectively. The K_m of (+)-**1** is increased 9-fold relative to that of the wild-type enzyme (Table 4). R395A shows a 30-fold increase for the same constant. As pointed out previously, R395K shows a surprising decrease in the apparent binding constant of Mg^{2+} (Table 1).

Mutation of Lys292 to glutamine resulted in a small effect on the turnover number and on the Michaelis constants for substrates and cofactors. The Michaelis constants for α-ketoglutarate (Table 3), ThDP (Table 1), and Mg^{2+} (Table 2) all decreased, while that for (+)-**1** (Table 4) increased ~4-fold. Again, the weaker binding of the artificial substrate allowed this change to be observable. The adjacent Arg293 was mutated to lysine, and this change had a <5-fold effect on the Michaelis constants of all the ligands, with no effect on α-ketoglutarate and a 3-fold decrease with respect to (+)-**1**.

Arg413 was replaced with lysine, and the resulting mutant showed a significant and specific effect on α-ketoglutarate (Table 3). The Michaelis constant increased 20-fold for this substrate, while remaining essentially constant for all other ligands. This also supports Dawson's modeled enzyme–intermediate complex.

Other Active-Site Residues: Ser32, Gln118, Ile418, Ser391, and Asp55. Several other residues at the active site predicted to participate in catalysis are shown in Figure 8. Ser32 is the analogue of Ser26 in benzoylformate decarboxylase (BFDC), which catalyzes the decarboxylation of benzoylformate to form benzaldehyde. This reaction is identical in nature to the first half-reaction catalyzed by MenD (Figure 2); the ThDP-bound anionic intermediate is simply protonated and released, rather than being used as a nucleophile. Crystal structures of BFDC with (*R*)-mandelate and methyl benzoylphosphonate (MBP) have been reported, which indicate Ser32 forms hydrogen bonds from the main chain and side chain heteroatoms to the carboxylate anion of mandelate and the phosphonate moiety of the ThDP–MBP adduct.[27] Crystallization of BFDC in the presence of benzoylphosphonic acid showed that Ser26 was phosphorylated by the substrate analogue.[32] In the case of acetohydroxy acid synthase (AHAS), which like MenD catalyzes a carboligase reaction, a glycine residue is found in this position. Interestingly, sequence alignment shows that this position is occupied by an aspartate residue in the enzyme pyruvate decarboxylase (PDC). When this residue was mutated to serine, the resulting mutant PDC was able to act as an AHAS-like carboligase that generated acetolactate as a product, indicating that this position is an arbiter of the fate of the postdecarboxylation anion. These results suggest that, by analogy, Ser32 of MenD would interact with the scissile carboxyl moiety of α-ketoglutarate. We generated the alanine and aspartate mutants of Ser32, predicting that both would strongly affect the interaction of α-ketoglutarate with the active site. In addition, we considered that S32D would result in a catalyst that protonated the succinyl-ThDP adduct in the absence of isochorismate, producing succinic semialdehyde.

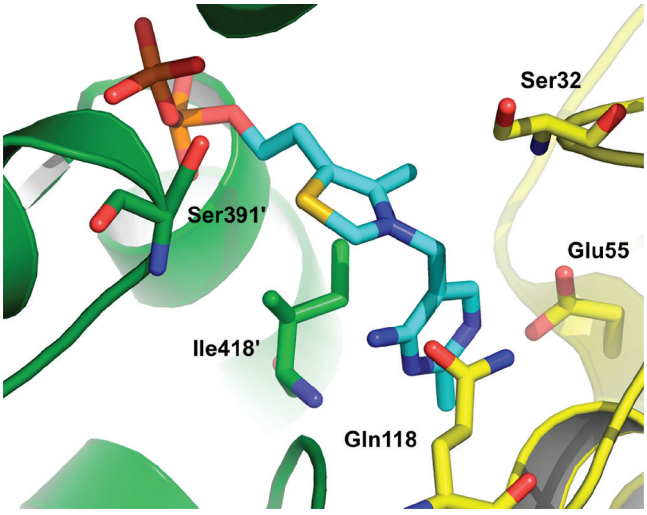

Figure 8. View of the active site of MenD. Monomers are shown with ribbon diagrams with carbon atoms colored yellow or green; ThDP is shown with carbon atoms colored cyan. Additional residues studied by mutagenesis are shown. Structure coordinates were from Protein Data Bank entry 2JLC. This figure was generated with MacPyMOL (Shrödinger LLC).

The kinetic constants for the S32A-catalyzed reaction of α-ketoglutarate and isochorismate are strikingly unchanged. The Michaelis constant of isochorismate remains too small to measure, and no other values have changed by a factor of >2. When **1** is used as a substrate, it seems that it is this substrate that is affected most by the mutation (Table 4). This suggestion is supported by the results observed for S32D. This mutant shows a greatly reduced apparent affinity for isochorismate (Table 4). As discussed previously, a high K_m value for isochorismate results in a UV absorbance for saturating concentrations of the substrate beyond the limit of the UV spectrophotometer, and the kinetic constants must be estimated by a Hanes–Woolf plot. The estimated k_{cat} value (9.5×10^{-3} min^{-1}) is 4 orders of magnitude lower than that of the wild type, and the estimated K_m value (260 μM) is at least 2 orders of magnitude higher. In the presence of **1**, only trace activity could be detected. We also tested S32D in the absence of isochorismate or **1** to see if succinate semialdehyde would be produced by protonation of the decarboxylated intermediate, but none could be detected by high-performance liquid chromatography or by addition of succinic semialdehyde dehydrogenase and $NADP^+$ (data not shown). We conclude that Ser32 of MenD plays an important role in the binding and/or reaction of isochorismate.

Gln118 is a strictly conserved residue among MenD sequences and is found at the active site. This residue has counterparts in homologous enzymes such as pyruvate oxidase (POX), benzaldehyde lyase (BAL), and AHAS.[17] Interestingly, this position is occupied by a histidine residue in other homologues, including BFDC.[33] We chose the isosteric Q118E substitution to test the role of this residue, on the grounds that a glutamate/glutamic acid residue might form hydrogen bonds and facilitate proton transfer, despite the very large pK_a difference. However, Q118E showed no detectable activity (using isochorismate or **1**). After our experiment was completed, a report of mutagenesis of the analogous Gln110 of AHAS appeared.[34] In this report, the Q110E mutant was also a sharply impaired catalyst, and the authors suggested that Gln110 formed a bridge between N4′ of the aminopyrimidine

ring and the ThDP−substrate adduct to facilitate proton transfer. In *E. coli* MenD, Gln118 is more than 4 Å from N4′ of ThDP, too far for a canonical hydrogen bond. Nevertheless, some movement upon substrate binding may allow this residue to fulfill a role similar to that proposed for Gln110 of AHAS.

Ile418 in MenD is located near ThDP with its uncharged side chain inserting between the aminopyrimidine ring and the thiazolium ring, as shown in Figure 8. All ThDP-dependent enzymes are believed to activate ThDP in essentially the same way, a conserved mechanism of tautomerization and ionization of the coenzyme via the "V conformation".[15] The enzyme-bound ThDP is held in this shape by the active site to bring the 4′-NH_2 and C2-H groups into proximity. Guo et al.[35] reported that residue Ile415 in PDC from *Saccharomyces cerevisiae* is located next to ThDP to enforce this conformation, and substitutions with methionine or leucine caused a great reduction in the k_{cat} value. Computational studies further indicated the large side chain of Ile415 reduces the flexibility of ThDP. The identity of the hydrophobic residue varies among ThDP-dependent homologues [pyruvate oxidase (POX) and AHAS use methionine for this purpose, but BFDC uses leucine], but the strategy appears to be consistent. It was therefore predicted that Ile418 in MenD plays the same role as Ile415 in PDC.

Changing this isoleucine residue to leucine in MenD caused a 20-fold increase in the K_m of α-ketoglutarate (Table 3), a 10-fold increase in the K_m of Mg^{2+} (Table 2), and a 75-fold increase in the K_m of ThDP (Table 1). Unlike the only ∼3% residual activity observed for PDC I415L, MenD I418L exhibited a turnover number similar to that of the wild-type enzyme using isochorismate or **1**. The observation that the catalytic specificity of ThDP was lowered by 2 orders of magnitude strongly supports the idea that this highly conserved residue is important for cofactor binding and activation in MenD, as expected. The small effects on the kinetic constants with respect to (+)-**1** (Table 4) underscore the independence of the binding and turnover of the second substrate.

Sequence alignments of MenD homologues revealed that a serine residue was strictly conserved, but this residue was not conserved among homologues such as AHAS, BFDC, and PDC. This residue, Ser391, was one of two conserved polar amino acids found in a stretch of hydrophobic residues, the other being Arg395 (discussed above). This region of the protein corresponds to a region of AHAS shown to interact with the second substrate of that reaction. We therefore hypothesized that this residue and Arg395 might interact with bound isochorismate.[12] Since the determination of the MenD structure, we subsequently noted that Ser391 aligns structurally with His260 of the α-ketoglutarate dehydrogenase complex E1 subunit (KGDHC E1). This histidine residue was shown by Frank et al. to be essential for catalysis.[36] Because KGDHC catalyzes a quite different set of reactions subsequent to decarboxylation, there was no clear hypothesis for the role of Ser391. The ThDP-bound MenD structure was ambiguous in this regard, because Ser391 is within 3 Å of both the sulfur atom of ThDP and an oxygen atom of the cofactor's β-phosphate. We have already discussed the effects of mutating Ser391 to alanine.[23] Briefly, the mutation has very little effect on the kinetic constants with respect to the cofactors and substrates. Of course, we could not determine what effect there was on the Michaelis constant of isochorismate, only that the value was not increased by a large factor. Using our synthetic substrate, we could determine the effect on binding of (+)-**1**, as shown in Table 4. We have confirmed that the S391A mutant has very similar catalytic properties with respect to all substrates and cofactors.

Glu55, a strictly conserved residue of MenD, was predicted to be essential for activation of ThDP. In the widely accepted mechanism for ThDP activation, a glutamic acid residue interacts with N1′ of the aminopyrimidine moiety, allowing tautomerization of this group, and abstraction of the C2-H proton. Sequence alignment identified Glu55 as the likely candidate for this role,[12] and we have reported that E55Q showed no detectable activity. We therefore generated E55D to determine the effects of a more conservative substitution of this residue. Unlike the significant reduction in catalytic activity observed for the IPDC E52D mutant,[37] E55D showed only slightly reduced activity; however, the catalytic specificity with respect to ThDP is 4-fold smaller (Table 1), and a similar effect was observed for Mg^{2+} (Table 2). This result supports the proposed role of Glu55 in the activation with ThDP. These relatively weak effects on binding of the cofactor result in essentially no effect on the substrate turnover; the kinetic constants with respect to α-ketoglutarate, isochorismate, and (+)-**1** are virtually unchanged (Tables 3 and 4).

CONCLUSION

The study of MenD has been hampered in the past by assumptions, chief among them the assumption that the product of the reaction was SHCHC, rather than SEPHCHC. With that lesson in mind, the development of substrate analogues **1** and **2** allowed us to generate experimental data to test the hypotheses and assumptions we currently hold about MenD. Specifically, we have used an artificial substrate and a dead-end inhibitor to demonstrate that MenD follows a ping-pong kinetic mechanism. Furthermore, we have been able to test many of the hypotheses generated from the published computational models of substrate binding. While we confirmed many of the assumptions held by ourselves and others, we have been able to exploit the weaker apparent binding of (+)-**1** to generate new information regarding the roles of active-site residues.

AUTHOR INFORMATION

Corresponding Author

*Telephone: (306) 966-4662. Fax: (306) 966-4730. E-mail: dave.palmer@usask.ca.

Funding

This work was supported by an NSERC Discovery Grant to D.R.J.P.

ACKNOWLEDGMENTS

We thank the Saskatchewan Health Research Foundation for funding the Molecular Design Research Group of the University of Saskatchewan, Dr. David Sanders (University of Saskatchewan) for helpful discussions and shared equipment, the staff of the Saskatchewan Structural Sciences Centre for many technical contributions, and Blaine Langman, Karen Ho, and Dan Toogood.

ABBREVIATIONS

AHAS, acetohydroxyacid synthase; BFDC, benzoylformate decarboxylase; DXPS, 1-deoxy-D-xylulose 5-phosphate synthase; IPDC, indolepyruvate decarboxylase; KGDHC, α-ketoglutarate dehydrogenase complex; PDC, pyruvate decarboxylase; POX,

pyruvate oxidase; SEPHCHC, 2-succinyl-5-enolpyruvyl-6-hydroxy-3-cyclohexene-1-carboxylate; SHCHC, 2-succinyl-6-hydroxy-2,4-cyclohexadiene-1-carboxylate; ThDP, thiamine diphosphate.

REFERENCES

(1) Jiang, M., Cao, Y., Guo, Z. F., Chen, M. J., Chen, X. L., and Guo, Z. H. (2007) Menaquinone biosynthesis in *Escherichia coli*: Identification of 2-succinyl-5-enolpyruvyl-6-hydroxy-3-cyclohexene-l-carboxylate as a novel intermediate and re-evaluation of MenD activity. *Biochemistry 46*, 10979−10989.

(2) Meganathan, R. (2001) Biosynthesis of menaquinone (vitamin K-2) and ubiquinone (coenzyme Q): A perspective on enzymatic mechanisms. *Vitam. Horm. (San Diego, CA, U.S.) 61*, 173−218.

(3) Wayne, L. G. (1994) Dormancy of *Mycobacterium tuberculosis* and latency of disease. *Eur. J. Clin. Microbiol. Infect. Dis. 13*, 908−914.

(4) Weinstein, E. A., Yano, T., Li, L. S., Avarbock, D., Avarbock, A., Helm, D., McColm, A. A., Duncan, K., Lonsdale, J. T., and Rubin, H. (2005) Inhibitors of type II NADH:menaquinone oxidoreductase represent a class of antitubercular drugs. *Proc. Natl. Acad. Sci. U.S.A. 102*, 4548−4553.

(5) Dhiman, R. K., Mahapatra, S., Slayden, R. A., Boyne, M. E., Lenaerts, A., Hinshaw, J. C., Angala, S. K., Chatterjee, D., Biswas, K., Narayanasamy, P., Kurosu, M., and Crick, D. C. (2009) Menaquinone synthesis is critical for maintaining mycobacterial viability during exponential growth and recovery from non-replicating persistence. *Mol. Microbiol. 72*, 85−97.

(6) Kurosu, M., Narayanasamy, P., Biswas, K., Dhiman, R., and Crick, D. C. (2007) Discovery of 1,4-dihydroxy-2-naphthoate prenyltransferase inhibitors: New drug leads for multidrug-resistant Gram-positive pathogens. *J. Med. Chem. 50*, 3973−3975.

(7) Lu, X. Q., Zhang, H. N., Tonge, P. J., and Tan, D. S. (2008) Mechanism-based inhibitors of MenE, an acyl-CoA synthetase involved in bacterial menaquinone biosynthesis. *Bioorg. Med. Chem. Lett. 18*, 5963−5966.

(8) Li, X. K., Liu, N. N., Zhang, H. N., Knudson, S. E., Slayden, R. A., and Tonge, P. J. (2010) Synthesis and SAR studies of 1,4-benzoxazine MenB inhibitors: Novel antibacterial agents against *Mycobacterium tuberculosis*. *Bioorg. Med. Chem. Lett. 20*, 6306−6309.

(9) Fang, M., Toogood, R. D., Macova, A., Ho, K., Franzblau, S. G., McNeil, M. R., Sanders, D. A. R., and Palmer, D. R. J. (2010) Succinylphosphonate Esters Are Competitive Inhibitors of MenD That Show Active-Site Discrimination between Homologous α-Ketoglutarate-Decarboxylating Enzymes. *Biochemistry 49*, 2672−2679.

(10) Palaniappan, C., Sharma, V., Hudspeth, M. E. S., and Meganathan, R. (1992) Menaquinone (vitamin-K2) biosynthesis: Evidence that the *Escherichia coli* MenD gene encodes both 2-succinyl-6-hydroxy-2,4-cyclohexadiene-1-carboxylic acid synthase and α-ketoglutarate decarboxylase activities. *J. Bacteriol. 174*, 8111−8118.

(11) Palaniappan, C., Taber, H., and Meganathan, R. (1994) Biosynthesis of o-succinylbenzoic acid in *Bacillus subtilis*: Identification of MenD mutants and evidence against the involvement of the α-ketoglutarate dehydrogenase complex. *J. Bacteriol. 176*, 2648−2653.

(12) Bhasin, M., Billinsky, J. L., and Palmer, D. R. J. (2003) Steady-state kinetics and molecular evolution of *Escherichia coli* MenD [(1*R*,6*R*)-2-succinyl-6-hydroxy-2,4-cyclohexadiene-1-carboxylate synthase], an anomalous thiamin diphosphate-dependent decarboxylase-carboligase. *Biochemistry 42*, 13496−13504.

(13) Jiang, M., Chen, M. J., Cao, Y., Yang, Y. H., Sze, K. H., Chen, X. L., and Guo, Z. H. (2007) Determination of the stereochemistry of 2-succinyl-5-enolpyruvyl-6-hydroxy-3-cyclohexene-1-carboxylate, a key intermediate in menaquinone biosynthesis. *Org. Lett. 9*, 4765−4767.

(14) Jiang, M., Chen, X. L., Guo, Z. F., Cao, Y., Chen, M. J., and Guo, Z. H. (2008) Identification and characterization of (1R,6R)-2-succinyl-6-hydroxy-2,4-cyclohexadiene-1-carboxylate synthase in the menaquinone biosynthesis of *Escherichia coli*. *Biochemistry 47*, 3426−3434.

(15) Jordan, F. (2003) Current mechanistic understanding of thiamin diphosphatedependent enzymatic reactions. *Nat. Prod. Rep. 20*, 184−201.

(16) Duggleby, R. G. (2006) Domain relationships in thiamine diphosphate-dependent enzymes. *Acc. Chem. Res. 39*, 550−557.

(17) Frank, R. A. W., Leeper, F. J., and Luisi, B. F. (2007) Structure, mechanism and catalytic duality of thiamine-dependent enzymes. *Cell. Mol. Life Sci. 64*, 892−905.

(18) Eubanks, L. M., and Poulter, C. D. (2003) *Rhodobacter capsulatus* 1-deoxy-D-xylulose 5-phosphate synthase: Steady-state kinetics and substrate binding. *Biochemistry 42*, 1140−1149.

(19) Sisquella, X., de Pourcq, K., Alguacil, J., Robles, J., Sanz, F., Anselmetti, D., Imperial, S., and Fernandez-Busquets, X. (2010) A single-molecule force spectroscopy nanosensor for the identification of new antibiotics and antimalarials. *FASEB J. 24*, 4203−4217.

(20) Cook, P. F., and Cleland, W. W. (2008) *Enzyme Kinetics and Mechanism*, Garland Science, New York.

(21) Cornish-Bowden, A. (2004) *Fundamentals of Enzyme Kinetics*, 3rd ed., Portland Press, London.

(22) Rusnak, F., Liu, J., Quinn, N., Berchtold, G. A., and Walsh, C. T. (1990) Subcloning of the enterobactin biosynthetic gene EntB: Expression, purification, characterization, and substrate-specificity of isochorismatase. *Biochemistry 29*, 1425−1435.

(23) Fang, M. H., Langman, B. M., and Palmer, D. R. J. (2010) A stable analog of isochorismate for the study of MenD and other isochorismate-utilizing enzymes. *Bioorg. Med. Chem. Lett. 20*, 5019−5022.

(24) Dawson, A., Chen, M. J., Fyfe, P. K., Guo, Z. H., and Hunter, W. N. (2010) Structure and Reactivity of *Bacillus subtilis* MenD Catalyzing the First Committed Step in Menaquinone Biosynthesis. *J. Mol. Biol. 401*, 253−264.

(25) Cornish-Bowden, A. (1995) *Analysis of Enzyme Kinetic Data*, Oxford University Press, New York.

(26) Kluger, R., and Pike, D. C. (1977) Active-site generated analogs of reactive intermediates in enzymic reactions: Potent inhibition of pyruvate-dehydrogenase by a phosphonate analog of pyruvate. *J. Am. Chem. Soc. 99*, 4504−4506.

(27) Brandt, G. S., Kneen, M. M., Chakraborty, S., Baykal, A. T., Nemeria, N., Yep, A., Ruby, D. I., Petsko, G. A., Kenyon, G. L., McLeish, M. J., Jordan, F., and Ringe, D. (2009) Snapshot of a reaction intermediate: Analysis of benzoylformate decarboxylase in complex with a benzoylphosphonate inhibitor. *Biochemistry 48*, 3247−3257.

(28) Arjunan, P., Sax, M., Brunskill, A., Chandrasekhar, K., Nemeria, N., Zhang, S., Jordan, F., and Furey, W. (2006) A thiamin-bound, pre-decarboxylation reaction intermediate analogue in the pyruvate dehydrogenase E1 subunit induces large scale disorder-to-order transformations in the enzyme and reveals novel structural features in the covalently bound adduct. *J. Biol. Chem. 281*, 15296−15303.

(29) Bunik, V. I., Denton, T. T., Xu, H., Thompson, C. M., Cooper, A. J. L., and Gibson, G. E. (2005) Phosphonate analogues of α-ketoglutarate inhibit the activity of the α-ketoglutarate dehydrogenase complex isolated from brain and in cultured cells. *Biochemistry 44*, 10552−10561.

(30) Dawson, A., Fyfe, P. K., and Hunter, W. N. (2008) Specificity and reactivity in menaquinone biosynthesis: The structure of *Escherichia coli* MenD (2-succinyl-5-enolpyruvyl-6-hydroxy-3-cyclohexadiene-1-carboxylate synthase). *J. Mol. Biol. 384*, 1353−1368.

(31) Priyadarshi, A., Kim, E. E., and Hwang, K. Y. (2009) Structural and functional analysis of vitamin K-2 synthesis protein MenD. *Biochem. Biophys. Res. Commun. 388*, 748−751.

(32) Bera, A. K., Polovnikova, L. S., Roestamadji, J., Widlanski, T. S., Kenyon, G. L., McLeish, M. J., and Hasson, M. S. (2007) Mechanism-based inactivation of benzoylformate decarboxylase, a thiamin diphosphate-dependent enzyme. *J. Am. Chem. Soc. 129*, 4120−4121.

(33) Tittmann, K., and Wille, G. (2009) X-ray crystallographic snapshots of reaction intermediates in pyruvate oxidase and transketolase illustrate common themes in thiamin catalysis. *J. Mol. Catal. B: Enzym. 61*, 93−99.

(34) Vyazmensky, M., Steinmetz, A., Meyer, D., Golbik, R., Barak, Z., Tittmann, K., and Chipman, D. M. (2011) Significant Catalytic Roles for Glu47 and Gln 110 in All Four of the C-C Bond-Making and -Breaking Steps of the Reactions of Acetohydroxyacid Synthase II. *Biochemistry 50*, 3250−3260.

(35) Guo, F. S., Zhang, D. Q., Kahyaoglu, A., Farid, R. S., and Jordan, F. (1998) Is a hydrophobic amino acid required to maintain the reactive V conformation of thiamin at the active center of thiamin diphosphate-requiring enzymes? Experimental and computational studies of isoleucine 415 of yeast pyruvate decarboxylase. *Biochemistry 37*, 13379−13391.

(36) Frank, R. A. W., Price, A. J., Northrop, F. D., Perham, R. N., and Luisi, B. F. (2007) Crystal structure of the E1 component of the *Escherichia coli* 2-oxoglutarate dehydrogenase multienzyme complex. *J. Mol. Biol. 368*, 639−651.

(37) Schutz, A., Golbik, R., Konig, S., Hubner, G., and Tittmann, K. (2005) Intermediates and transition states in thiamin diphosphate-dependent decarboxylases. A kinetic and NMR study on wild-type indolepyruvate decarboxylase and variants using indolepyruvate, benzoylformate, and pyruvate as substrates. *Biochemistry 44*, 6164−6179.